Effects of hydrogen bonds on solid state TATB, RDX, and DATB under high pressures*

Guo Feng(郭 峰)[a)b)c)†], Zhang Hong(张 红)[d)], Hu Hai-Quan(胡海泉)[a)b)], and Cheng Xin-Lu(程新路)[c)]

[a)] *School of Physical Science and Information Technology, Liaocheng University, Liaocheng* 252000, *China*
[b)] *Shandong Provincial Key Laboratory of Optical Communication Science and Technology, Liaocheng* 252000, *China*
[c)] *Institute of Atomic and Molecular Physics, Sichuan University, Chengdu* 610065, *China*
[d)] *School of Physical Science & Technology, Sichuan University, Chengdu* 610065, *China*

(Received 23 March 2013; revised manuscript received 29 October 2013; published online 20 February 2014)

To probe the behavior of hydrogen bonds in solid energetic materials, we conduct ReaxFF and SCC–DFTB molecular dynamics simulations of crystalline TATB, RDX, and DATB. By comparing the intra- and inter-molecular hydrogen bonding rates, we find that the crystal structures are stabilized by inter-molecular hydrogen bond networks. Under high-pressure, the inter- and intra-molecular hydrogen bonds in solid TATB and DATB are nearly equivalent. The hydrogen bonds in solid TATB and DATB are much shorter than in solid RDX, which suggests strong hydrogen bond interactions existing in these energetic materials. Stretching of the C–H bond is observed in solid RDX, which may lead to further decomposition and even detonation.

Keywords: hydrogen bond, TATB, RDX, DATB, ReaxFF, energetic materials

PACS: 65.40.–b, 82.20.Wt, 82.30.–b, 82.30.Rs **DOI:** 10.1088/1674-1056/23/4/046501

1. Introduction

The safety and effective destructibility of energetic materials (EMs) are hot topics at the moment because of their potential applications in various fields. In the past decade, researchers have found that the sensitivity of EM is related to the bond dissociation energy (BDE) of the weakest bond, such as C–NO_2 and N–NO_2.[1–10] Stephen *et al.*[11] confirmed that the C–NO_2 bond is the weakest bond in 1, 3, 5-triamino-2, 4, 6-trinitrobenzene (TATB) molecule, and further discussed that aromatic Car–Car bonds are also notably weak. Researchers[12–17] found that the C–NO_2 bond plays a key role in the early stage of decompositions of EMs. However, recent studies also suggested that inter-molecular interactions can affect the sensitivity of energetic material. Yang *et al.*[18] found that the cocrystal of 2, 4, 6, 8, 10, 12-hexanitrohexaazaisowurtzitane (HNIW) and 2, 4, 6-trinitrotoluene (TNT) exhibits low impact sensitivity. The cocrystal of 2, 4, 6, 8, 10, 12-hexanitro-2, 4, 6, 8, 10, 12-hexaazaiso-wurtzitane (CL-20) and 1, 3, 5, 7-tetranitro-1, 3, 5, 7-tetrazacy-clooctane (HMX) shows higher power while lower sensitivity.[19] Zhang *et al.*[20] suggested that the π-stacked structure in a 1, 3, 5-triamino-2, 4, 6-trinitrobenzene (TATB) crystal could offer an energetic buffer against external mechanical stimuli. Ojeda and Çağın[21] found a molecular rearrangement that is caused by the strong hydrogen bond between neighboring atoms. Through molecular dynamics simulations, Kohno *et al.*[22] found that the 1, 3-diamino-2, 4, 6-trinitrobenzene (DATB) molecules are linked by inter-molecular hydrogen bonds into continuous chains along *a* axis. Around 67 GPa, Manaa and Fried[23] found that intra- and inter-molecular hydrogen bonds (–$NO_2\cdots H_2N$–) in solid TATB become nearly equivalent. Many studies[24–30] proved that the hydrogen bond plays an important role in solid-state materials under high-pressure. To explore the relation between hydrogen bond and sensitivity of EMs, we study the hydrogen bond phenomena of solid-state EMs at various pressures.

2. Simulation details

2.1. Potential

In this current work, London dispersion corrected reactive force field (ReaxFF-lg)[31] and self-consistent charges-density functional tight binding (SCC–DFTB) method[32,33] are employed. ReaxFF[34] is a potential based on quantum mechanics, which can be used to simulate chemical reactions of materials. In the ReaxFF, the general relationship between bond distance and bond order is used, and the dissociation and formation of bonds can be described properly. The DFTB method with self-consistent charges is derived by expanding the Kohn–Sham density function theory (DFT) expression of total energy to second order in charge fluctuation $\delta\rho(r)$ around ρ_0. The parameter that needs to be fitted is the repulsive pair potential $V_{\rm rep}$. As long as $V_{\rm rep}$ is properly fitted with *ab initio* data set, SCC–DFTB calculations can well maintain the accuracy of the DFT method.

*Project supported by the National Natural Science Foundation of China (Grant No. 11176020) and the Fund from the China Academy of Engineering Physics, China (Grant No. 2011A0302014).

†Corresponding author. E-mail: gfeng.alan@foxmail.com

© 2014 Chinese Physical Society and IOP Publishing Ltd

2.2. Crystal structures and simulation method

The bulk TATB is a supercell of 4×4×4 containing 3072 atoms. The lattice parameters are taken from Cady' value:[35] $a = 9.01$ Å, $b = 9.03$ Å, $c = 6.81$ Å, $\alpha = 108.59°$, $\beta = 91.82°$, and $\gamma = 119.97°$. The supercell (2×2×2) of cyclotrimethylene trinitramine (RDX) contains 1344 atoms. Initial positions are taken from experimental data: $a = 13.182$ Å, $b = 11.574$ Å, and $c = 10.709$ Å, $\alpha = \beta = \gamma = 90.0°$.[31] The lattice parameters of DATB cube are $a = 7.309$ Å, $b = 5.169$ Å, and $c = 11.583$ Å, $\alpha = \gamma = 90.0°$ and $\beta = 95.22°$, which are cited from X-ray diffraction measurement in Ref. [22]. The simulation slab of DATB is a 4×4×4 supercell containing 2816 atoms. The depictions of unit cell and molecular structures are available in Fig. 1.

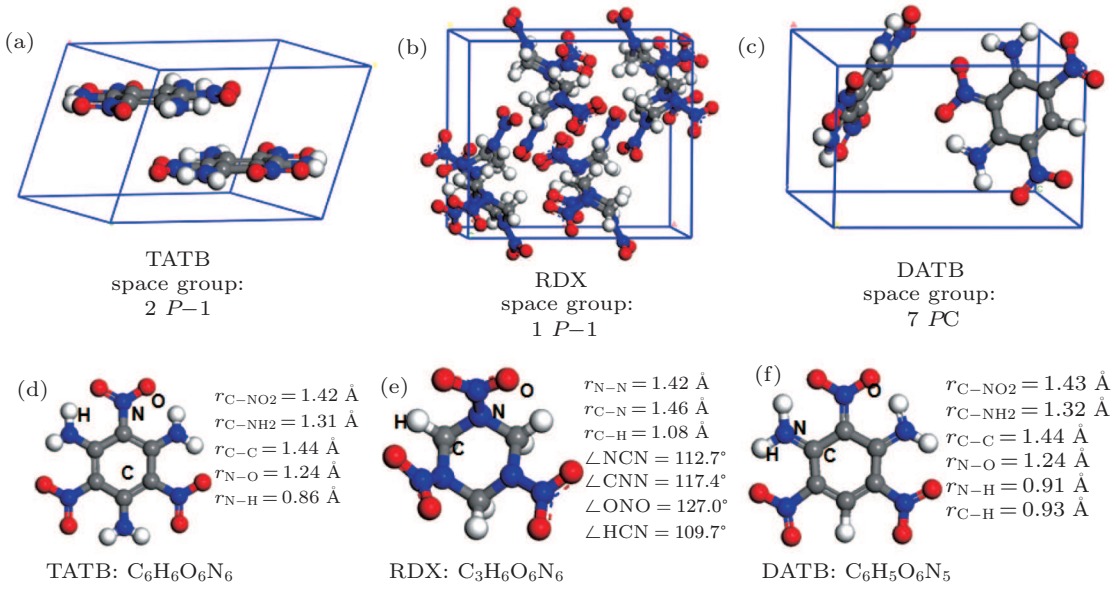


Fig. 1. (color online) Unit cells of (a) TATB, (b) RDX, and (c) DATB. The bulk structures of TATB, RDX, and DATB used in the simulations are super cells of 4×4×4, 2×2×2, and 4×4×4, respectively. The molecular structure and bond/angle information are shown in (d) TATB, (e) RDX, and (f) DATB. The bond and angle information are cited from Refs. [35], [36], and [22].

To fully relax the bulk structure of the EMs (see Fig. 2), low temperature molecular dynamics (MD) are investigated. The RDX crystal is cooled down to $T = 10$ K using a temperature scale constant of 50 fs with isothermal–isobaric (NPT) ensemble. After thermal relaxations, a series of NPT-MD simulations at various pressures is carried out. The total time of each simulation is 10.0 ps, and three-dimensional periodic conditions are used. All simulations in time steps of 0.1 fs to give a better description of the dynamic process.

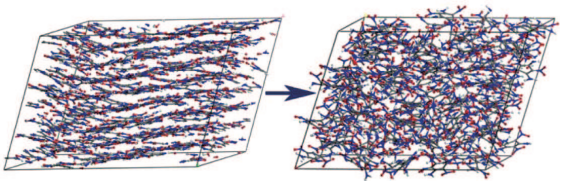


Fig. 2. (color online) Crystal structure transferred from crimped layered structure to the disordered structure under temperature 2500 K. Snapshot times of these two figures are 100.0 fs and 5.0 ps, respectively.

SCC–DFTB calculations are taken with dftb+ package.[32,33] Conjugate gradient and velocity Verlet algorithm are used for geometry optimization and MD simulations, respectively. The Anderson charge mixing method is used with a mixing constant of 0.05. The Lennard–Jones dispersion model with universal force field (UFF) parameters is used to properly describe the hydrogen bond interactions.

2.3. A computer program for finding hydrogen bond structures in MD trajectories

To study the role of hydrogen bonding (HB) in EMs under high-pressure, a complete analysis of the entire molecular-dynamic (MD) trajectory is necessary. Although there are already open source programs to do this task, such as VMD[37] and Hbonanza,[38], they are used to analyze HB in the protein structure or alike, and can be tedious when they are used to identify and analyze HB in crystal structures of EMs such as TATB, RDX and DATB.

In our computer code, the HB (Fig. 3) is defined[39,40] by the following criteria: (i) the candidate of HB acceptor is oxygen, nitrogen or carbon atoms; (ii) the distance between the acceptor atom and proton is less than the sum of the van der Waals radii[1,41] of the acceptor and proton; and, (iii) the angle of acceptor–H–donor is bigger than 120°.

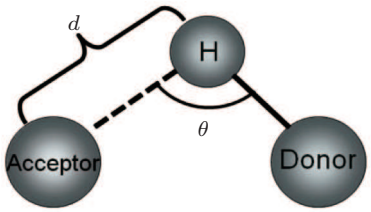


Fig. 3. (color online) A schematic plot of the hydrogen bond structure, where d is defined as the distance between the acceptor and proton, and θ is the angle between acceptor–H bond and atom–donor bond.

The hydrogen bonding rate (HBR) is further defined to give hydrogen bond a quantitative description under different conditions. The formula of intra-molecular and inter-molecular HBR can be expressed by the following formulae:

$$\mathrm{HBR_{intra}} = \frac{\text{intra-molecular hydrogen bonds}}{\text{total H atoms}}, \quad (1)$$

$$\mathrm{HBR_{inter}} = \frac{\text{inter-molecular hydrogen bonds}}{\text{total H atoms}}. \quad (2)$$

And the total HBR can be expressed by

$$\mathrm{HBR_{total}} = \mathrm{HBR_{intra}} + \mathrm{HBR_{inter}}.$$

3. Result and discussion

Before further investigations, we test the accuracy of ReaxFF-lg parameter set[31] and the standard parameter set of the SCC–DFTB method by comparing our results with existing *ab initio* or experimental data. The isothermal equation of state (EOS) of TATB crystal (see Fig. 4) of SCC–DFTB calculations is in good agreement with the result in Manaa and Fried's work[23] in the low pressure range, but is underestimated under high pressure conditions. Compared with the result in Conroy *et al.*'s work,[42] the isothermal EOS is underestimated by the SCC–DFTB method, but well agrees with Olinger *et al.*'s value.[43] No experimental results or *ab initio* data of the EOS of the DATB crystal are available for comparison. Lattice parameters calculated in the present work, and those from existing experiments and *ab initio* calculations are listed in Table 1. Further validations of ReaxFF of nitro energetic materials are available in Refs. [43]– [47].

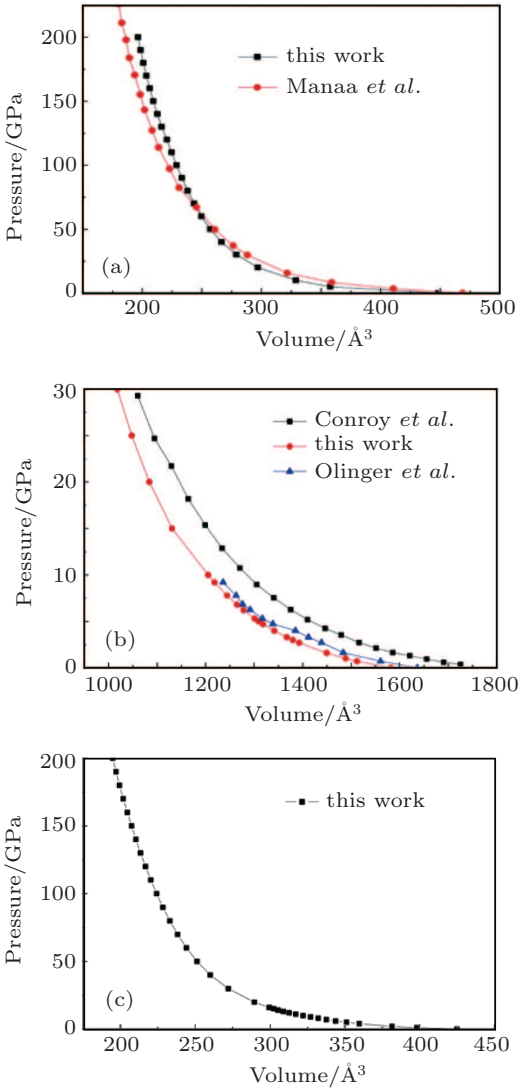


Fig. 4. (color online) (a) Isothermal EOS of TATB compared with Manaa's work, (b) isothermal EOS of RDX compared with Conroy and Olinger's results, and (c) isothermal EOS of DATB crystal up to 200 GPa.

Table 1. Comparisons between experimental and computational unit cell lattice parameters of TATB, RDX, and DATB crystals (cell dimension in Å and angles in degree). In SCC–DFTB calculations standard SK parameters are cited from the www.dftb.org website, and in the ReaxFF calculations the ReaxFF-lg parameter set is used.

	Method	a	b	c	α	β	γ
TATB	exp[a]	9.010	9.028	6.812	108.58	91.82	119.97
	DFT[b]	9.219	9.181	7.161	107.7	92.0	120.2
	SCC–DFTB	8.992	8.990	8.166	121.77	91.519	119.835
	ReaxFF	8.8401	8.8348	6.1315	108.05	78.29	119.82
DATB	exp[c]	7.309	5.169	11.583	90.0	95.22	90.0
	SCC–DFTB	7.332	5.384	10.871	90.0	98.1	90.0
	ReaxFF	7.053	4.987	11.177	90.0	95.22	90.0
RDX	Expd	13.182	11.574	10.709	90.0	90.0	90.0
	DFT[e]	13.522	11.758	11.102	90.0	90.0	90.0
	SCC–DFTB	13.435	11.139	10.570	90.0	90.0	90.0
	ReaxFF	13.477	11.049	10.476	90.0	90.0	90.0

[a]Experimental X-ray results are cited from Ref. [35], [b]DFT(GGS-PBE) calculations from Ref. [23], [c]X-ray diffraction measurements from Ref. [22], [d]X-ray diffraction experimental results from Ref. [48], and [e]PBE-DFT calculations from Ref. [39].

3.1. Hydrogen bond rates in TATB, RDX, and DATB crystal

Intra- and inter-molecular hydrogen bonding rates are calculated according to formulae (1) and (2). The mean hydrogen bonding rate is obtained by averaging the ReaxFF-MD simulations over thermal equilibrium steps (Fig. 5). Crystals TATB and DATB each have a higher total hydrogen bonding rate. The intermolecular HBR is rising when the pressure is increasing in all crystals; however, the total HBR of TATB is nearly unchanged and the intra-molecular HBR tend to decrease, which indicates that the inter-molecular hydrogen bonds are formed, instead of intra-molecular hydrogen bonds, to stabilize the crystal structure when pressure is higher. As shown in Fig. 4(c), almost no inter-molecular hydrogen bonds exist in RDX crystal. Intra- and inter-molecular HBR in TATB and RDX show linear correlation with pressure, except DATB under a pressure between 5.0 GPa to 10.0 GPa, and both the inter- and intra-molecule HBR behave strangely with pressure changing. Kohno *et al.*[22] observed a structural change under pressure between 7.5 GPa∼8.5 GPa in their calculations. To explain this strange behavior in the DATB crystal structure, we study the pressure–volume (P–V) and pressure–energy (P–E) relationship of DATB crystal by the SCC–DFTB method. However, the P–V relation in Figure 4(c) shows no abnormal points around 7.5 GPa∼8.5 GPa, which suggest no phase transitions or structural changes in this region.

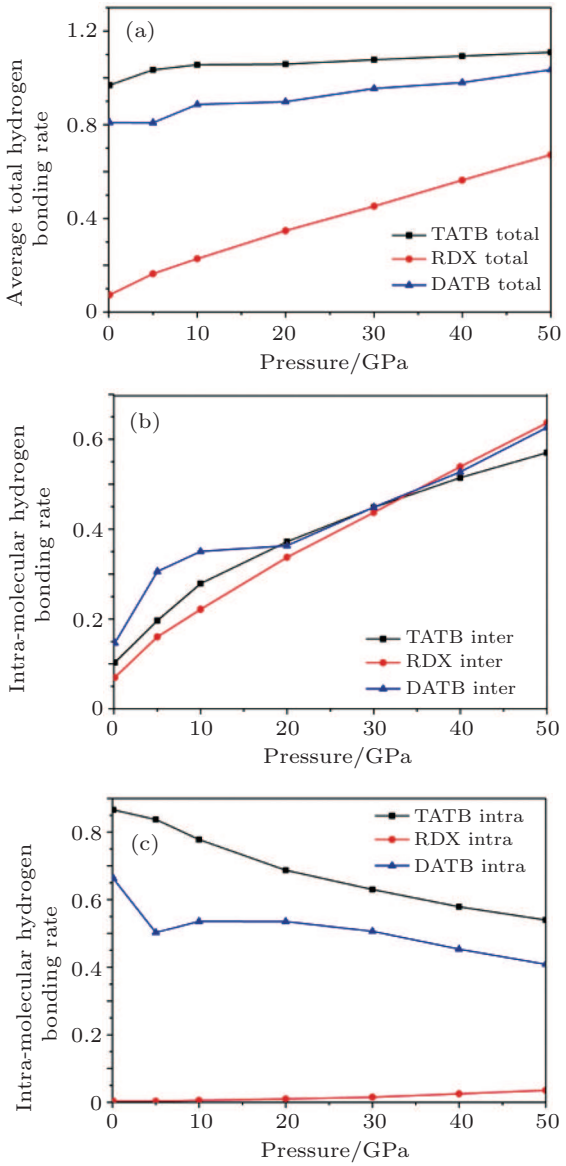


Fig. 5. (color online) Average total, intermolecular, and intramolecular hydrogen bonding rate each as a function of pressure in (a) TATB crystal, (b) RDX crystal, and (c) DATB crystal, respectively. The time of each simulation is 10.0 ps. These MD simulations are carried out with ReaxFF force field.

3.2. Hydrogen-bond structures

Hydrogen bonding structures in TATB, RDX, and DATB are shown in Figure 6. Figure 6(a) shows the close ring structures formed between two adjacent TATB molecules in the same crystal layer under a pressure of 60.0 GPa. The lengths of the intra-molecular hydrogen bond range from 1.690 Å to 1.975 Å, while inter-molecular hydrogen bonds are in a range from 1.854 Å to 1.906 Å. Figure 6(b) shows that two TATB molecules form a hydrogen bond ring structure, and forms N–H···N hydrogen bond with the molecule in the under layer, the bond lengths of H···O and H···N are 1.847, 1.853, and 1.874 Å, respectively. Nearly equivalent inter- and intra-molecular hydrogen bond lengths in TATB crystal under a pressure of about 60.0 GPa are in good agreement with Manaa and Fried's[23] calculations under hydrostatic compressions. Figure 6(c) shows two protons of amino group hydrogen bonded

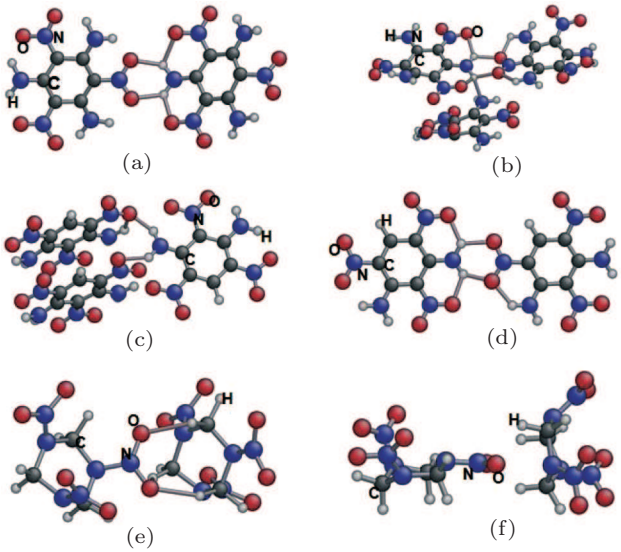


Fig. 6. (color online) (a) Close ring structure with hydrogen bonds connected. (b) Two TATB molecules formed hydrogen bond ring structure, while at the same time one H forms H···N–O hydrogen bond with a molecule in the under layer. (c) Protons in one amino group hydrogen bond with O atoms belonging to two nitro groups. (d) Hydrogen bond ring structure formed in DATB crystal. (e) Hydrogen bond structure in RDX crystal. (f) The bending of the $-NO_2$ group towards a neighboring RDX molecule. Red represents O, white H, gray C, and blue N, respectively. These structures are all taken from SCC–DFTB calculations of crystal structure of TATB, RDX, and DATB under pressure of 60.0 GPa.

with nearing O atoms in two nitro groups. Figure 6(d) shows that the neighboring nitro and amino group can also form hydrogen bond ring structure in DATB crystal. Hydrogen bond lengths in Figure 6(c) are 1.753 Å and 1.728 Å, in Figure 6(d) are 1.699 and 1.820 Å, and these values are similar to those of TATB crystal. Hydrogen bond structures in our calculations are also in good accordance with Kohno *et al.*'s results.[22] They classified the DATB molecule into two groups: one is the group that adjoins two amino groups, and the other is the group that adjoins one amino group and aromatic proton as shown in Figs. 6(c) and 6(d). Figure 6(e) shows the hydrogen bond network between RDX molecules, and the hydrogen bond lengths are 1.792, 1.829, and 1.922 Å, respectively. Figure 6(f) shows that one of the three nitro groups in RDX bends toward a neighboring molecule, the plane angle is about 147.031°, and the lengths of $-NO_2\cdots H$ is 1.756 Å and 1.841 Å, respectively.

3.3. Inter- and intra-molecular pair distribution function of –H···X

The radius distribution functions (represented by $g(r)$) are shown in Fig. 7. The first peak of the intra-molecular $g(r)$ function represents the average C–H bond length. Figure 7 indicates that in TATB and DATB the C–H bond lengths are around 1.07 Å under 0.1 GPa, and 1.03 Å under 50 GPa by ReaxFF calculations, and 1.03 Å under 60 GPa by the SCC–DFTB calculations. The C–H bond lengths in RDX are around 1.13 Å under 0.1 GPa and 1.12 Å by ReaxFF, and 1.11 Å under 60 GPa by SCC–DFTB calculations.

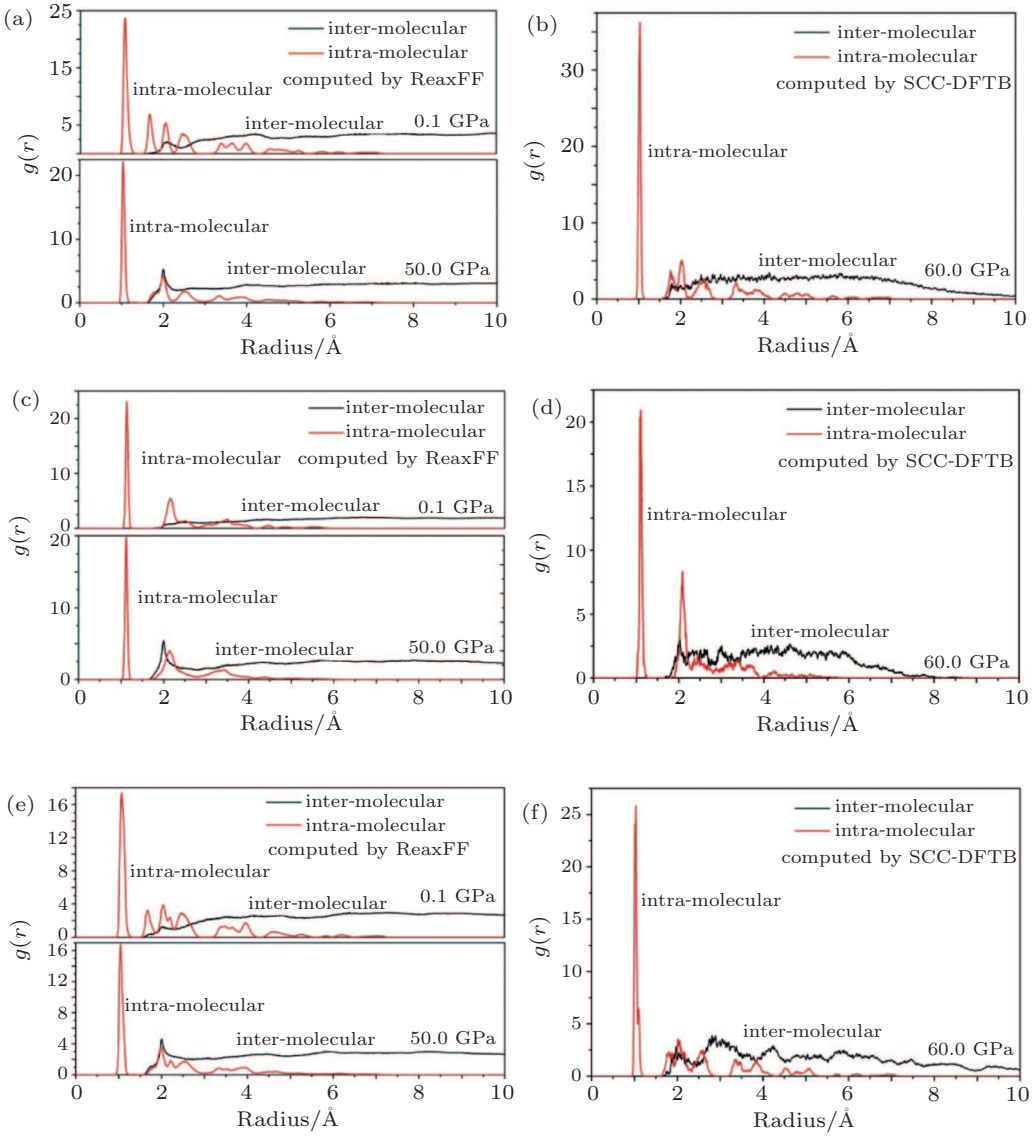


Fig. 7. (color online) Inter- and intra-molecular pair distribution functions between –H···X. (a) A comparison of the $g(r)$ of the TATB crystal between under pressure 0.1 GPa and under pressure 50.0 GPa, computed by ReaxFF-MD. (b) The $g(r)$ of TATB computed by SCC–DFTB. (c) A comparison of the $g(r)$ of the RDX crystal between under pressure 0.1 GPa and under pressure 50.0 GPa, computed by ReaxFF–MD. (d) The $g(r)$ of RDX computed by SCC–DFTB. (e) A comparison of $g(r)$ of DATB crystal between under pressure 0.1 GPa and under pressure 50.0 GPa, computed by ReaxFF–MD. (f) The $g(r)$ of RDX computed by SCC–DFTB.

Under high pressure conditions (up to 50 GPa) the first peak of inter-molecular and the second peak of intra-molecular $g(r)$ functions are nearly overlapped, which indicates that the TATB and DATB crystals tend to form shorter inter- and intra-molecular hydrogen bonds in a highly compressed state. With pressure ranging from 0.1 GPa to 50 GPa, the intra-molecular bond lengths in solid TATB and DATB are distributed from 1.65 Å to 1.99 Å by ReaxFF calculations, and 1.78 Å under 60 GPa by SCC–DFTB calculations. The inter-molecular bond length is in a range from 2.07 Å to 2.00 Å in ReaxFF calculations, while in SCC–DFTB calculations it is around 1.85 Å. While in solid state RDX, the intra-molecular hydrogen bond lengths are around 2.16 Å and 2.09 Å in ReaxFF and SCC–DFTB calculations respectively, a much larger value than those in solid TATB and DATB, and only slightly changed under compression conditions.

The nearly equivalent inter- and intra-molecular hydrogen bond lengths in solid TATB and DATB by SCC–DFTB calculations are in good agreement with Manaa and Fried's calculations,[23] but they have a deviation from ReaxFF calculations in predicting hydrogen bonding length under high pressure region (ReaxFF gives a large value, around 2.0 Å).

3.4. Electronic properties of crystalline TATB, DATB, and RDX

The evolutions of the valence-conduction energy gap as a function of pressure are shown in Fig. 8. Our results are in quantitative agreement with the band gap value estimated by Kalar *et al.*[49], which is computed from X-ray-absorption spectrum (XAS) and core-level and valence-band photo-electron spectra (VBPES). Wu *et al.*[50] indicated that the metallization pressure (the gap value went to zero) of TATB is 120 GPa computed by LDA DFT; however, it far exceeds a known detonation pressure of TATB (30 GPa).

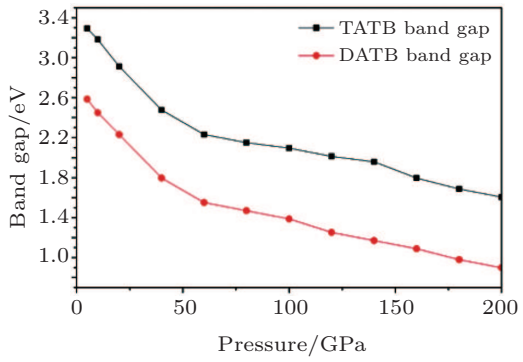


Fig. 8. (color online) Plots of energy gap between valence and conduction band versus pressure.

The mean charges under different pressures of TATB, RDX, and DATB are listed in Table 2. It can be obviously seen that the charges of H atoms are increased by 0.03–0.05 due to the formation of hydrogen bond (–H···ON–), and the charges of O atoms have slightly decreased. Hydrogen bonds are strengthened by the increased induced dipole–dipole interaction between H and O atoms.

Table 2. The average charge population of TATB, RDX, and DATB (pressure is in GPa).

Atom	Pressure	TATB	RDX	DATB
C	0.0	-0.002	0.103	–0.016
	60.0	–0.012	–0.002	–0.013
H	0.0	0.238	0.110	0.227
	60.0	0.288	0.143	0.256
N	0.0	0.306	0.396	0.435
	60.0	0.280	0.437	0.411
O	0.0	–0.542	–0.557	–0.535
	60.0	–0.556	–0.579	–0.544

4. Conclusion

We conducted ReaxFF and SCC–DFTB MD simulations of TATB, RDX, and DATB bulks under various pressures to investigate the behaviors of the hydrogen bonds of energetic materials. Through analysis of the hydrogen bonding rate as a function of pressure, we found that as pressure changes the total HBRs of TATB and DATB are only slightly changed at a high level, which indicates a large number of hydrogen bonds, even at lower pressures. In response to further compression, part of intra-molecular hydrogen bonds in TATB and DATB are opened and thus form inter-molecular hydrogen bonds. Compared with the total HBRs of TATB and DATB, the total HBR of RDX crystal has a rapid increase as pressure rises and only a few intra-molecular hydrogen bonds exist in RDX. In high pressure regions, we further note that: i) the lengths of inter- and intra-molecular hydrogen bond of TATB and DATB are nearly equivalent, but shorter than that of crystalline RDX; and, ii) the bond stretching exists in solid RDX if the C–H bond length of RDX is much longer than those of TATB and DATB, which will lead to proton transfer reactions and even detonation. The electronic structure calculations show that the hydrogen bond interactions are strengthened by the charge transfers between neighboring O and H atoms.

References

[1] Rice B M and Hare J J 2001 *J. Phys. Chem. A* **106** 1770
[2] Zhang H, Cheung F and Zhao F 2009 *Int. J. Quantum Chem.* **109** 1547
[3] Melius C F 1990 *Chemistry and Physics of Energetic Materials* (Amsterdam: The Netherlands)
[4] Politzer P, Murray J S and Struct J M 1996 *J. Mol. Struct.* **376** 419
[5] Politzer P and Murray J S 1995 *Mol. Phys.* **86** 251
[6] Politzer P, Murray J S and Concha M C 1998 *J. Phys. Chem. A* **102** 6697
[7] Shao J X, Cheng X L, Yang X D and He B 2006 *Chin. Phys.* **15** 329
[8] Wu C J and Fried L E 1998 "First-principles Study of High Explosive Decomposition Energetics" in: *Elventh International Detonation Symposium*, Snowmass, Colorado, USA, p. 490
[9] Fried L E, Manaa M R, Pagoria P F and Simpson R L 2001 *Ann. Rev. Mater. Res.* **31** 291
[10] Liu H, Zhao J J, Gong Z Z, Ji G F and Wei D Q 2007 *Phys. Lett. A* **367** 383

[11] Stephen A D, Srinivasan P and Kumaradhas P 2011 *Comput. Theor. Chem.* **967** 250

[12] Politzer P and Murray J S 2003 *Energetic Materials Part* 2*: Detonation and Combustion, Theoretical and Computational Chemistry* (Amsterdam: Elsevier B V) p. 174

[13] Owens F J 1996 *J. Mol. Struct.* (Theochem) **370** 11

[14] Muray J S and Politzer P 1990 *Chem. Phys. Lett.* **168** 135

[15] Rice B M, Samir S and Owens F J 2002 *J. Mol. Struct.* (Theochem) **583** 69

[16] Xiao H M, Fan J F and Gong X D 1997 *Propellants, Explosives, Pyroechnics* **22** 360

[17] Zhi C Y Cheng X L and Zhao F 2010 *Propellants, Explosives, Pyroechnics* **35** 555

[18] Yang Z W, Li H Z, Huang H, Zhou X Q, Li J S and Nie F D 2010 *Propellants, Explosives, Pyroechnics* **35** 1

[19] Bolton O, Simke L R, Pagoria P H and Matzger A J 2012 *Cryst. Growth Des.* **12** 4311

[20] Zhang C Y, Wang X C and Huang H 2008 *J. Am. Chem. Soc.* **130** 8359

[21] Ojeda O U and Çğın T 2011 *J. Phys. Chem. B* **115** 12085

[22] Kohno Y, Hiyoshi R I, Yamaguchi Y, Matsumoto S, Koseki A, Takahashi O, Yamasaki K and Ueda K 2009 *J. Phys. Chem. A* **113** 2551

[23] Manaa M R and Fried L E 2012 *J. Phys. Chem. C* **116** 2116

[24] Ren X P, Zhou B, Li L T and Wang C L 2013 *Chin. Phys. B* **22** 016801

[25] Li D F, Gao S Q, Sun C L and Li Z W 2012 *Chin. Phys. B* **21** 083301

[26] Ouyang S L, Wu N N, Sun C L, Liu J Y, Li Z W and Gao S Q 2010 *Chin. Phys. B* **19** 093103

[27] Chen M, Min R, Zhou J M, Hu H, Lin B, Miao L and Jiang J J 2010 *Acta Phys. Sin.* **58** 5148 (in Chinese)

[28] Chen C Z, Li P, Lin X Y, Liu C Q, Qiu S H, Wu Y D and Yu C Y 2009 *Acta Phys. Sin.* **58** 2565 (in Chinese)

[29] Zhang Z H, Han K, Li H P, Tang G, Wu Y X, Wang H T and Bai L 2008 *Acta Phys. Sin.* **57** 3160 (in Chinese)

[30] Zhao X Y, Wang H, Yan H, Gai Z, Zhao R G and Yang W S 2001 *Chin. Phys.* **16** 392

[31] Liu L, Liu Y, Zybin S V, Sun H and Goddard W A 2011 *J. Phys. Chem. A* **115** 11016

[32] Aradi B, Hourahine B and Frauenheim T 2007 *J. Phys. Chem. A* **111** 5678

[33] Elstner M, Suhai S and Seifert G 1998 *Phys. Rev. B* **58** 7260

[34] van Duin A C T, Dasgupta S, Lorant F and Goddard W A 2001 *J. Phys. Chem. A* **105** 9396

[35] Cady H H and Larson A C 1965 *Acta Cryst.* **18** 485

[36] Borges I, Aquino A J A, Barbatti M and Lischka H 2009 *Int. J. Quantum Chem.* **109** 2348

[37] Humphrey W, Dalke A and Schulten K 1996 *J. Mol. Grap.* **14** 33

[38] Durrant J D and McCammon J A 2011 *J. Mol. Grap. Model.* **31** 5

[39] Scheiner S 1997 *Hydrogen Bonding: A Theoretical Perspective* (Oxford: Oxford University Press)

[40] Guo F, Zhang H and Cheng X L 2009 *J. Theor. Comp. Chem.* **9** 315

[41] Bondi A 1964 *J. Phys. Chem.* **68** 441

[42] Conroy M W, Oleynik I I, Zybin S V and White C T 2008 *J. Appl. Phys.* **104** 113501

[43] Olinger B, Roof B and Cady H 1978 *Symposium on High Dynamic Pressures*, Paris, France, p. 3

[44] Zhou T T and Huang F L 2011 *J. Phys. Chem. B* **115** 278

[45] Zhang L, Zybin S V, van Duin A C T, Dasgupta S and Goddard W A 2009 *J. Phys. Chem. A* **113** 10619

[46] Strachan A, van Duin A C T, Chakraborty D, Dasgupta S and Goddard W A 2003 *Phys. Rev. Lett.* **91** 098301

[47] Strachan A, Kober E M, van Duin A C T, Oxgaard J and Goddard W A 2005 *J. Chem. Phys.* **122** 054502

[48] Choi C S and Prince E 1972 *Acta Cryst. B* **28** 2857

[49] Kakar S, Nelson A J, Treusch R, Heske C, Buuren T V, Jimenez I, Pagoria P and Terminello L J 2000 *Phys. Rev. B* **62** 15666

[50] Wu C J, Yang L H and Fried L E 2003 *Phys. Rev. B* **67** 235101